Cluster measurements of rapidly moving sources of ELF/VLF chorus

U. S. Inan, M. Platino, and T. F. Bell
STAR Laboratory, Stanford University, Stanford, California, USA

D. A. Gurnett and J. S. Pickett
Department of Physics and Astronomy, University Of Iowa, Iowa City, Iowa, USA

Received 14 October 2003; revised 5 February 2004; accepted 26 February 2004; published 14 May 2004.

[1] The first simultaneous measurements of discrete chorus emissions on multiple spacecraft, realized in the context of the Cluster mission, revealed a rather unexpected frequency difference of around 1 kHz between nearly identical discrete elements observed on different spacecraft [*Gurnett et al.*, 2001]. This frequency difference is interpreted herein as a natural outcome of the dependence of the whistler-mode refractive index on the wave normal angle between the wave vector **k** and the static magnetic field $\mathbf{B}_0$ and the rapid motion of highly localized source region(s) of chorus of 400 km to 1700 km in extent along the field line, but only less than 100 km transverse to the magnetic field, and moving at speeds of 20,000 km/s to 25,000 km/s. Wave packets emanating from the localized regions propagate to two spacecraft at different wave normal angles, and are observed at different frequencies due to the differential Doppler shift between the two spacecraft. These differences in frequency, as well as the different times of arrival of the similar emissions at the different spacecraft, provide a unique opportunity to estimate the source characteristics, using a model involving rapidly moving sources traveling at speeds comparable to the parallel resonant velocity of counterstreaming electrons moving along the Earth's magnetic field lines. We report the determination of chorus emission source region motion for two different cases observed during 2000–2001, where these differences in frequency were readily observable due to the relatively large separation of the Cluster spacecraft. We also report a case in 2002 where the spacecraft separations were smaller, so that these frequency differences were not as evident but nevertheless measurable. In general, our results provide the first experimental evidence that the sources that generate the discrete chorus emissions are in rapid motion. *INDEX TERMS:* 2730 Magnetospheric Physics: Magnetosphere—inner; 2768 Magnetospheric Physics: Plasmasphere; 6939 Radio Science: Magnetospheric physics; 6984 Radio Science: Waves in plasma; *KEYWORDS:* chorus waves, multipoint measurement of chorus, sources of chorus

Citation: Inan, U. S., M. Platino, T. F. Bell, D. A. Gurnett, and J. S. Pickett (2004), Cluster measurements of rapidly moving sources of ELF/VLF chorus, *J. Geophys. Res.*, *109*, A05214, doi:10.1029/2003JA010289.

1. Introduction

[2] Discrete ELF/VLF chorus emissions constitute the most intense form of electromagnetic plasma waves observed in the vicinity of the Earth [*Smith et al.*, 1996; *Inan et al.*, 1992; *Lauben et al.*, 1998] and other magnetized planets [*Scarf et al.*, 1979; *Warwick et al.*, 1979; *Gurnett et al.*, 1979a]. Prior to the Cluster mission, most of the past observations of ELF/VLF chorus have been on single spacecraft [*Lauben et al.*, 2002, and references therein], although there was a large amount of simultaneous chorus data collected from the ISEE 1 and 2 spacecraft [*Gurnett et al.*, 1979b]. Simple comparison of chorus spectrograms from ISEE 1 and 2 indicated that the size of the wave packets responsible for the chorus emissions was probably less than a few hundred kilometers. In all of the data looked at from ISEE 1 and 2, it was generally not possible to find a one-to-one correlation between any of the chorus elements, probably because the separation between spacecraft was too large, typically ranging from several hundred to several thousand kilometers.

[3] The first simultaneous observations of chorus emissions on multiple Cluster satellites produced surprising results, with the same individual elements observed at different frequencies on different spacecraft [*Gurnett et al.*, 2001]. In the present paper, we provide a natural interpretation of these observations by invoking rapid motion of the compact source region(s) of chorus, which leads to the observed frequency differences due to the dependence of the whistler-mode refractive index on the wave normal angle between the wave vector **k** and the static magnetic field $\mathbf{B}_0$. It

0148-0227/04/2003JA010289$09.00

is important to note that the rapid motion of chorus source regions is not inconsistent with any aspect of our basic theoretical understanding of chorus being emitted as a result of gyroresonance interactions with counterstreaming energetic electrons. In fact, the drift motion of the chorus interaction region was discussed explicitly by *Helliwell* [1967], observing that such drifts could occur either in the direction of chorus propagation or opposite to it, and at speeds ranging from zero to the wave group velocity or the parallel velocity of the resonant electrons.

2. Theory and Methodology

[4] Before we introduce specific observations and their quantitative interpretation, we consider in general the Doppler shifts that would be expected to result from source region motion and illustrate how this effect would lead to the observation of individual wave packets (emanating from the same source region) at different frequencies on two different spacecraft. We then describe the method by which we can use the measured values of differential Doppler shift and time delay to determine the location of the chorus source region.

2.1. Doppler Shift of Whistler-Mode Waves Due to Motion of Compact Sources

[5] Consider a compact source located at $z_s = s(t)$, $x_s = 0$, emitting waves at a frequency $\omega(t)$ while moving along $\mathbf{B}_0$ at a speed $v_s = \partial s/\partial t$ in a uniform (homogeneous) medium. For simplicity we consider a two dimensional space with the z axis along $\mathbf{B}_0$ and the x axis perpendicular to $\mathbf{B}_0$. The signal phase $\phi(\psi, t)$ observed on a spacecraft located at x, z is given by

$$\phi(\psi,t) = \int \omega(t)dt - k_x(\psi,t)\,x - k_z(\psi,t)\,[z - s(t)] \qquad (1)$$

where ψ is the wave normal angle, i.e., the angle between the **k**-vector and the static magnetic field $\mathbf{B}_0$. The observed frequency is thus given by

$$\omega'(\psi,t) \simeq \omega(t) - \underbrace{\left[\frac{x}{v_{gx}(\psi,t)} - \frac{z - s(t)}{v_{gz}(\psi,t)}\right]\frac{\partial\omega}{\partial t}}_{\text{Normal Propagation Delay}} + \underbrace{k_z(\psi,t)\frac{\partial s(t)}{\partial t}}_{\text{Doppler Shift}} \qquad (2)$$

where we neglect spacecraft motion and assume that the wave normal angle ψ remains constant over a relatively short propagation path from the source to the observer. The spacecraft motion can be neglected for normal spacecraft velocities (~5 km/sec), since the Doppler shift due to spacecraft motion is very small for refractive indices of <500. As illustrated in Figure 1a, waves emanating from a compact source can reach two different observers SC1 and SC2 only by propagating at two different wave normal angles ψ_1 and ψ_2, and are thus observed at two different 'apparent' frequencies ω_1' and ω_2', with the frequency difference (or the differential Doppler shift) $\Delta\omega$ is given by

$$\Delta\omega = \omega_1' - \omega_2' = [k_z(\psi_1,t) - k_z(\psi_2,t)]\frac{\partial s(t)}{\partial t} \qquad (3)$$

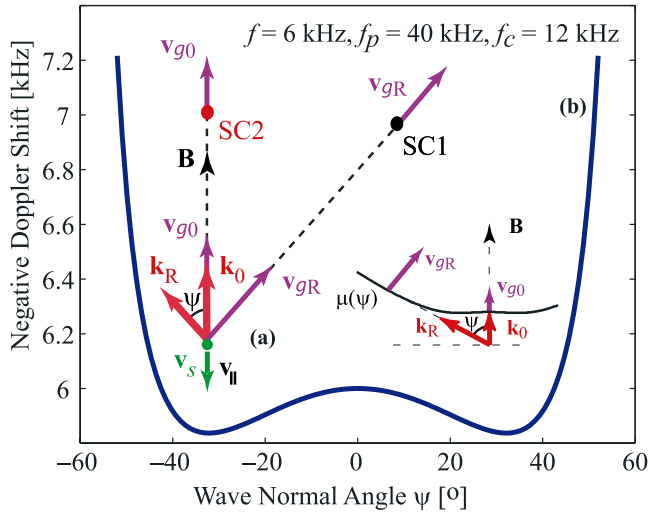

Figure 1. Placement of the source location with respect to the Cluster spacecraft and calculated Doppler shift as a function of the wave normal angle ψ. This calculation corresponds to a plasma frequency of 40 kHz and an electron gyrofrequency of 12 kHz. Results are shown for a source frequency of 6 kHz and for a source velocity assumed (only for the purposes of this plot) to be equal to the parallel velocity of gyroresonant electrons. (Note that our analysis of the Cluster data shows the source velocities to be of the same order but somewhat lower in magnitude than $v_{\|}$.) Also shown are the refractive index surface and the corresponding orientations of the wave group velocities $\mathbf{v}_g$ and wave vector **k** at $\psi = 0$ (labeled $\mathbf{v}_{g0}$ and $\mathbf{k}_0$, respectively) and, for $\psi \sim \psi_R$, the resonance cone angle (labeled $\mathbf{v}_{gR}$ and $\mathbf{k}_R$, respectively).

It is evident from Figure 1b that the observed differential Doppler shift $\Delta\omega$ would be relatively small for the cases in which (i) the sources have large spatial extent, (ii) the sources are at large distances (compared to the spacing between observers) from the observers, and (iii) the two observers are close to one another (compared to the distance between them and the sources).

[6] Given the fact that the underlying mechanism for generation of ELF/VLF chorus is believed to be the cyclotron resonance interaction, with the velocity of the 'source' of the radiation likely being of the same order as the velocity of the counterstreaming electrons moving at the parallel resonant velocity $v_{\|}$, we may estimate the magnitude of the differential Doppler shift by assuming the source velocity to be given by the cyclotron resonance condition

$$v_s = -v_{\|} = \frac{\omega_c - \omega_0}{k_0} \simeq \frac{(\omega_c - \omega_0)^{3/2}}{\omega_p\,\omega_0^{1/2}} \qquad (4)$$

where ω_p and ω_c are the electron plasma and gyrofrequencies and $k_0 = k_z(\psi = 0)$. The subindex 0 refers to waves with **k** vector in the direction of the magnetic field line. (Note that this source velocity is adopted here solely for the purposes of an initial evaluation of the Doppler shift as shown in Figure 1; in our later analyses, we find the source velocities to be somewhat smaller than both $v_{\|}$ and the wave

group velocity v_g). From equation (4), the Doppler shift ω_d is then given by

$$\omega_d = -k_z v_s = -\frac{\omega\mu_z}{c}\left[\frac{(\omega_c-\omega_0)^{3/2}}{\omega_p\,\omega_0^{1/2}}\right] \simeq -\frac{\omega\mu\cos\psi}{c}\left[\frac{(\omega_c-\omega_0)^{3/2}}{\omega_p\,\omega_0^{1/2}}\right] \tag{5}$$

where ω refers to the frequency of the wave with $\mathbf{k}$ vector at an angle ψ with respect to the magnetic field line. The refractive index μ is given by Appleton-Hartree formula for whistler-mode waves [*Helliwell*, 1965, p. 23]

$$\mu^2 \simeq 1 - \frac{(\omega_p^2/\omega^2)}{1-\frac{\omega_c^2\sin^2\psi}{2(\omega^2-\omega_p^2)} - \left[\left(\frac{\omega_c^2\sin^2\psi}{2(\omega^2-\omega_p^2)}\right)^2 + \frac{\omega_c^2}{\omega^2}\cos^2\psi\right]^{\frac{1}{2}}} \tag{6}$$

The Doppler shift calculated using equations (3), (4), (5), and (6) for the case of $f_c = 12$ kHz, $f_p = 40$ kHz, and for $\omega_0/2\pi = f_c/2 = 6$ kHz is shown in Figure 1 as a function of wave normal angle ψ. Also shown plotted as a function of ψ is the magnitude of the refractive index μ. Noting that the cold plasma parameters chosen are representative of the Cluster observations presented in later sections, it is evident from Figure 1 that even for modest refractive index values (e.g., $|\mu| < 100$) Doppler shifts observed at different wave normal angles can differ by as much as ~1.2 kHz. The two observers SC1 and SC2 can thus observe waves originating from the same source at two frequencies differing from each other by as much as ~1.2 kHz, i.e., with a differential Doppler shift $\Delta\omega$ of ~1.2 kHz. Two observers SC1 and SC2 would in general observe any discrete chorus wave packets emitted at the source at slightly different times, in view of the known dependence of the whistler-mode group velocity on wave normal angle ψ. Such a differential time delay would in general be expected to be present whenever we observe a differential Doppler shift, although the reverse is not necessarily the case, noting that differential time delay would also be observed if both spacecraft were along the field line of the source (in which case they would observe the waves with identical Doppler shift) but displaced in the direction along the field line. It is also useful to note that a differential Doppler shift would result in those cases when the two observers SC1 and SC2 are displaced (with respect to one another) either in the radial or azimuthal direction, or both. The differential Doppler shift and time delay are only a function of the wave normal angle ψ.

2.2. Determination of Source Location and Speed From Measured Differential Doppler Shift and Time Delay

[7] Having shown that both a differential Doppler shift (Δf) and time delay (Δt) are natural consequences of the propagation of whistler-mode wave packets from a compact moving source to two differently spaced observers, we now describe the methodology we use to determine the source location and velocity from measurements of Δf and Δt. Consider a source located along the same field line as one of two satellites (SC2) as shown in Figure 2, so that waves emanating at $\mathbf{k}\|\mathbf{B}_0$ (i.e., $\psi = 0$) reach SC2 propagating with a refractive index and a group velocity v_{g0} given by

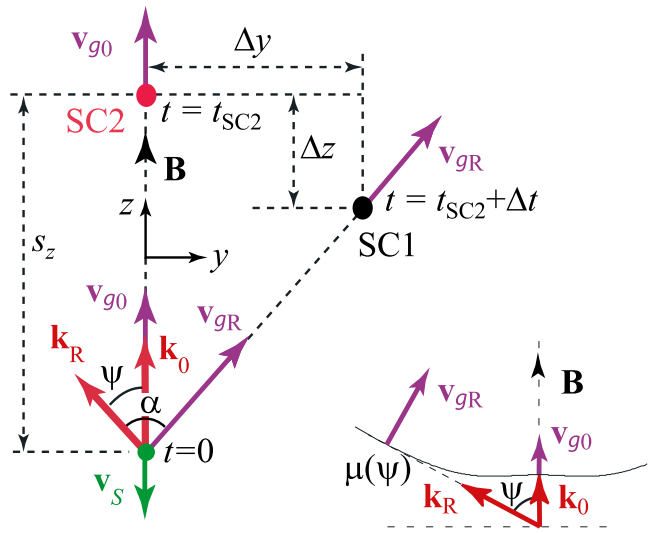

Figure 2. Parameters involved in the determination of the source location with respect to the Cluster spacecraft. Highlighted are the two spacecraft SC1 and SC2 as well as the pertinent vector magnitudes of group velocity $\mathbf{v}_{g0}$, wave vector $\mathbf{k}$, and source velocity $\mathbf{v}_s$. For the case shown, the wave arrives first at SC2 at $t = t_{SC2}$ and later at SC1 at time $t_{SC2} + t$.

$$\mu_0^2 = 1 - \frac{(\omega_p/\omega)^2}{1-(\omega_c/\omega)} \quad ; \quad v_{g0} \simeq 2\,c\,\omega^{1/2}\frac{[\omega_c-\omega]^{3/2}}{\omega_p\,\omega_c} \tag{7}$$

[8] The second satellite (SC1) is displaced in longitude and latitude as well as in L-shell, so that it is accessible from the same source only by waves emanating at a relatively large wave normal angle ψ, corresponding to a refractive index $\mu(\psi) > \mu_0$ given by equation (6). The magnitude of the source velocity v_s is then related to the measured differential Doppler shift (Δf) as

$$v_s = \frac{2\pi\Delta f}{\Delta k_z(\psi)} = \frac{c\,\Delta f}{(f\mu\cos\psi - f_0\mu_0)} \tag{8}$$

where $\Delta f = f - f_0$. The angle θ between the group velocity vector $\mathbf{v}_g(\psi)$ and $\mathbf{k}$ is given by

$$\theta \simeq \cos^{-1}\left\{\left[1-\frac{\omega}{\omega_c\cos\psi}\right]\left[\frac{\tan^2\psi}{4} + \left(1-\frac{\omega}{\omega_c\cos\psi}\right)^2\right]^{-\frac{1}{2}}\right\} \tag{9}$$

whereas the magnitude of the group velocity $v_g(\psi)$ is given by

$$v_g(\psi) \simeq \frac{2\,c\left(\frac{\omega}{\omega_c}\right)^{\frac{1}{2}}}{\left(\frac{\omega_p}{\omega_c}\right)}\left[\frac{\tan^2\psi\left(\cos\psi-\frac{\omega}{\omega_c}\right)}{4} + \frac{\left(\cos\psi-\frac{\omega}{\omega_c}\right)^3}{\cos^2\psi}\right]^{\frac{1}{2}} \tag{10}$$

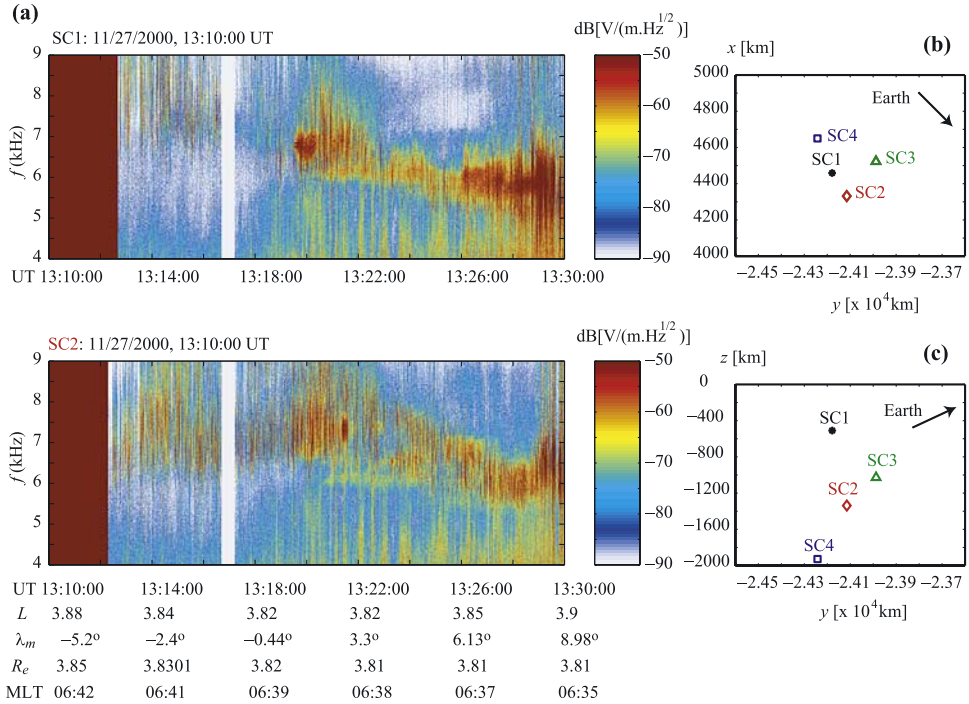

Figure 3. (a) WBD overview spectrogram of the Cluster satellite pass during November 27, 2000, starting at 13:10:00 UT. The magnitude scale refers to electric field amplitude with 0 dB corresponding to 1 V/m/$\sqrt{Hz}$. Also shown are the relative positions of the four spacecraft with each other and the corresponding distances to Earth. (b) The x coordinate represents the Earth-Sun axis, while the y coordinate is perpendicular to x, still lying in the Earth's orbit plane. The Sun is perpendicular to the page away from the reader. (c) The z coordinate is perpendicular to the orbital plane of the Earth.

Equations (9) and (10) are general expressions which can be applied to any wave at a frequency ω with a $\mathbf{k}$ vector at an angle ψ with respect to the magnetic field line. The parallel and perpendicular components of $\mathbf{v}_g(\psi)$ are given by

$$v_{g\parallel} = v_g \cos(\theta - \psi) \tag{11a}$$

$$v_{g\perp} = v_g \sin(\theta - \psi) \tag{11b}$$

The differential time delay Δt is then given by the set of equations

$$\Delta y = v_{g\perp}(\psi)\,(t_{SC2} + \Delta t) \tag{12a}$$

$$s_z = v_{g0}\, t_{SC2} \tag{12b}$$

$$s_z - \Delta z = v_{g\parallel}\,(t_{SC2} + \Delta t) \tag{12c}$$

where s_z is the distance from the spacecraft to the source located along the same field line, Δy is the separation of the satellite along the y axis, and Δz is the separation of the satellites along the z axis. With Δy and Δz known, together with f_c and f_p, we can solve the above equations iteratively until we find a source location (i.e., s_z) consistent with the measured time delay Δt. In all of the above equations, the quantities should be understood to be functions of frequency f, e.g., $t_{SC2}(f)$, etc.. The process can be repeated for each value of frequency f, to determine the various quantities as a function of f and compare with the observed dispersion of chorus elements. Such a comparison would in principle allow the determination of the frequency-time shape of chorus as emitted at the source. Note that the wave normal angle ψ for any given $\mu(\psi)$ can be readily determined from the relation [*Stix*, 1962, p. 12]

$$\tan^2\psi = -\frac{\varepsilon_\parallel[\mu^2 - (\varepsilon_\perp + \varepsilon_\times)][\mu^2 - (\varepsilon_\perp - \varepsilon_\times)]}{(\mu^2 - \varepsilon_\parallel)[\varepsilon_\perp\mu - (\varepsilon_\perp^2 - \varepsilon_\times^2)]} \tag{13}$$

where

$$\varepsilon_\perp = 1 - \frac{\omega_p^2}{\omega^2 - \omega_c^2} \quad ; \quad \varepsilon_\times = \left(\frac{\omega_c}{\omega}\right)\frac{\omega_p^2}{\omega^2 - \omega_c^2} \quad ; \quad \varepsilon_\parallel = 1 - \frac{\omega_p^2}{\omega^2} \tag{14}$$

3. Observations and Interpretation

[9] We now present three different sets of observations of discrete chorus emissions during perigee passes of the Cluster spacecraft in the vicinity of the geomagnetic equator near L 4. The separation distances between the spacecraft in these three cases are ~2530 km, ~840 km, and <110 km, respectively, with the differential Doppler shifts being accordingly different. The time resolution of the measurements is 1 msec, meaning that the measured delay between the two spacecraft can have up to 2 msec error. With the

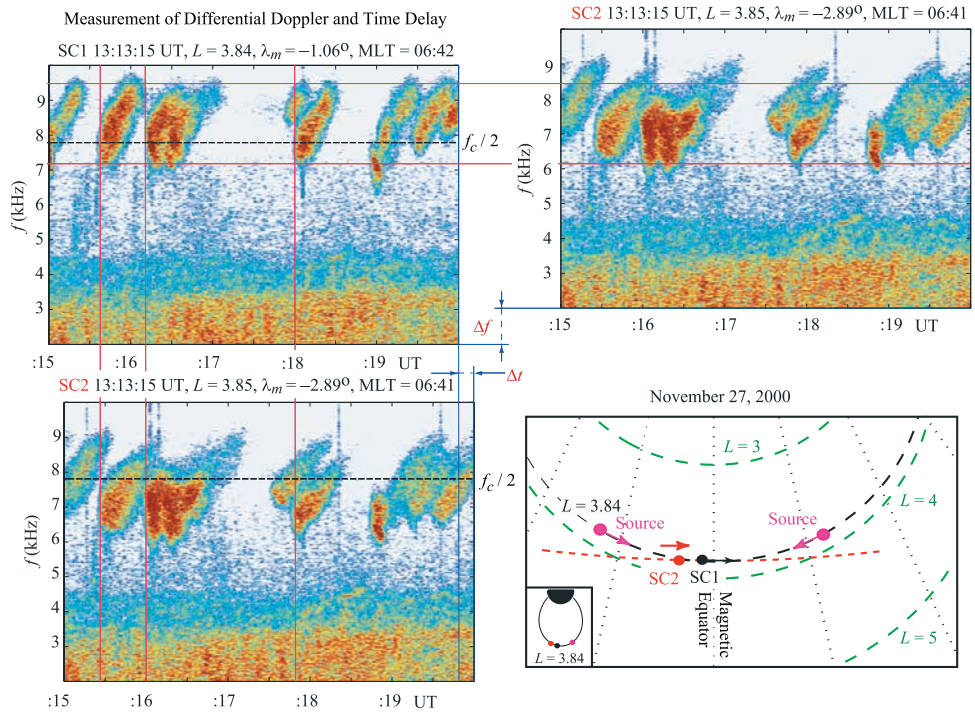

Figure 4. Expanded record of a 5-s-long data segment, starting at 13:13:15 UT, on November 27, 2000, showing a sequence of individual chorus elements observed on both SC1 and SC2. The magnitude scale refers to electric field amplitude with 0 dB corresponding to 1 V/m/$\sqrt{Hz}$. The SC2 panel is repeated on the right to illustrate the differential Doppler shift. Also shown in the bottom right panel is the location (not shown to scale) of the spacecraft with respect to the two possible source locations (as derived from our analysis) along the field line. The small panel on the bottom left of this diagram shows the entire field to provide perspective.

method of visual overlaying (described below) of 30-s-long spectrograms (produced with 50 Hz frequency resolution) used to measure Doppler shift and time delays (and to identify discrete chorus emissions common to both spacecraft among many others that are not), the measurements are estimated to be accurate to two significant digits, corresponding to an actual measurement error of ~10 msec.

3.1. Case 1: November 27, 2000

[10] Figure 3a shows frequency-time spectrograms showing chorus emissions observed with the Wideband (WBD) instrument [*Gurnett et al.*, 1997] on two Cluster spacecraft, referred to as SC1 and SC2, as they crossed the geomagnetic equatorial plane. The spacecraft separation at the time of this observation was ~2500 km, with the precise coordinates of the two spacecraft being as shown in Figures 3b and 3c. The general variations of the chorus frequency as observed on the two spacecraft are similar, but the frequency difference is evident, as was previously noted by *Gurnett et al.* [2001].

[11] Figure 4 shows an expanded record of a 5-s-long data segment, showing a sequence of individual chorus elements observed on both SC1 and SC2. The similarity of the temporal sequencing and frequency-time shapes of the emissions strongly suggests a common source, yet the frequency difference of Δf and the time difference (or time delay) of Δt are clearly evident. In fact, careful examination (Figure 5) also reveals that the frequency-time slopes of individual discrete chorus elements are discernibly different, as would be expected on the basis of the dependence of the dispersion of whistler-mode waves on the wave normal angle ψ. The local electron gyrofrequency is calculated on the basis of a centered dipole model of the Earth's magnetic field, and the spacecraft location as determined by the ephemeris.

[12] For the case in hand, the individual chorus elements are risers (i.e., their frequencies increase with time), so that the higher frequencies are likely to have been emitted at points later in time and thus closer to (or farther from) the observers, depending on whether the source is determined to be moving toward (or away from) the observers. Determination of the source location and velocity (both speed and the direction of motion relative to the observing spacecraft) starts by choosing the source location to be along the same field line as one of the observing spacecraft, with the other being displaced in radial distance (or azimuth) as shown in Figure 5a. This choice can be made solely on the basis of the differential time delay between the onsets of the individual elements observed on the two spacecraft, based on the fact that (for any given frequency) the group velocity for whistler-mode propagation is a maximum for $\psi = 0$. This assumption has to be tempered by the fact that the group velocity is frequency dependent and that the waves are observed at different frequencies on the two spacecraft; however, for the cases studied in this paper, the chorus frequencies lie in the vicinity of half the local electron

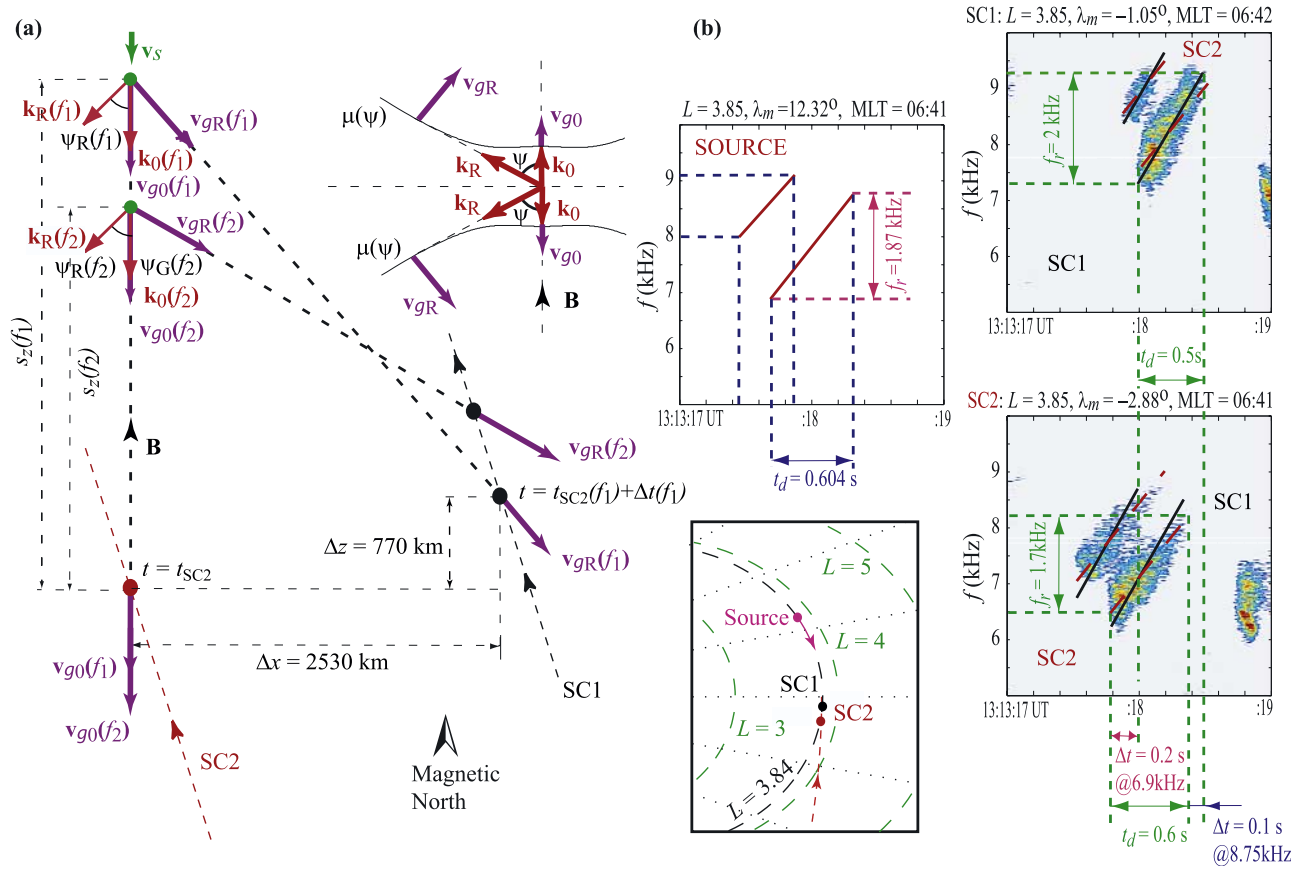

Figure 5. (a) Placement of the source position with respect to the spacecraft and the mechanism of propagation (from source to spacecraft) of chorus elements with increasing frequency (risers) on November 27, 2000, at 13:13:15 UT. Included is a plot of the refractive index surface at different wave normal angle values. (b) Detailed measurement of differential delay and Doppler shift leads to a calculated frequency-time shape at the source as shown in the left panel. This panel shows the results of the calculations of differential Doppler shift and time delay using the calculated values of refractive index and group velocity. Also shown is the location of the spacecraft with respect to the source along the field line.

gyrofrequency, for which the frequency variation of the group velocity is small. For the case in hand, the chorus elements are observed first on SC2 and then on SC1 (see Figure 4), so that the source is assumed to be along the same field line as SC2, as shown in Figure 5a. Note that this assumption is not in any way limiting in terms of our overall conclusions (i.e., that the sources of discrete chorus emissions are in rapid motion); indeed, assuming the source to be located at another field line (not necessarily that of SC1 or SC2) would simply result in smaller calculated differential Doppler shifts and would thus require somewhat larger source velocities to match the same observed differential Doppler shift.

[13] Once the source is placed along the same field line as one of the spacecraft (SC2 in this case) on the basis of the time delay measurement, the determination of the direction of the source region motion can be made based solely on the polarity of the differential Doppler shift, assuming that the differential Doppler shift is largely due to the difference in magnitudes of the refractive index (μ) rather than the geometric projection factor (i.e., $\cos\psi$), as is evident from Figure 1. For the case in hand, the magnitude of the Doppler shift is expected to be higher as observed on SC1 (since ψ, and thus the magnitude of the **k**-vector, is higher), and since the chorus elements are observed at a higher frequency on SC2, the polarity of the Doppler shift must be so as to decrease frequency (i.e., negative), thus indicating that the source region motion is toward the spacecraft. With the source chosen to lie along the same field line as SC2 and the direction of source region motion determined, the calculation of the location of origin of each frequency component and the magnitude of the source velocity involves a search through parameter space using equations (7)–(12) with the goal of finding a solution consistent with all measurables. In this context, we fully account for the measurably different frequency-time slope of the individual chorus elements as measured on the two spacecraft. The manner in which this measurement is used in our determination of the source properties is illustrated in Figure 5b. The discrete emission at the source is assumed to occur with a linearly increasing frequency with time (two such elements successively emitted at different starting frequencies are shown in the upper left panel of Figure 5b), and the emission then disperses (by a small but nevertheless measurable amount) to display the

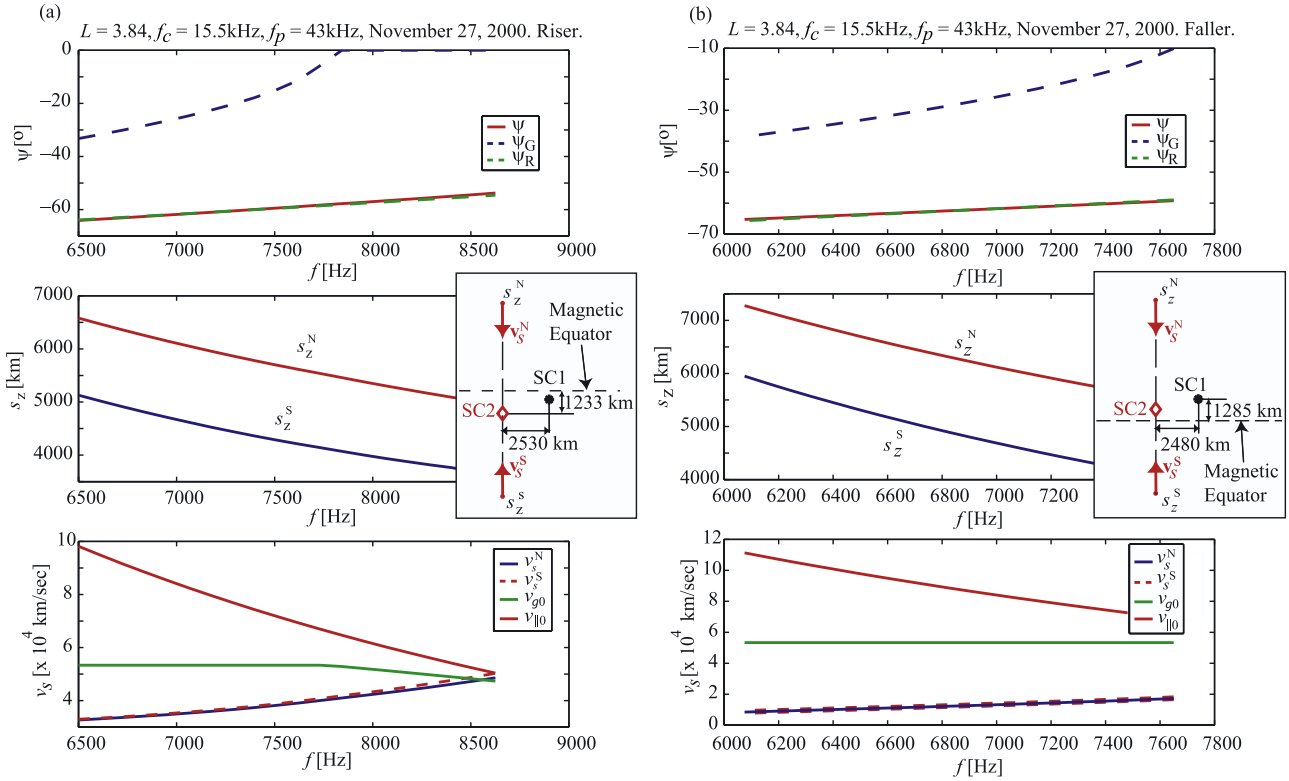

Figure 6. (a) Results of the calculations of the source location and source velocity as a function of frequency for the cases on November 27, 2000, at 13:13:15 UT. Shown are the two solutions, one with a source located north of the spacecraft and another with the source located south of the spacecraft. The corresponding values of wave normal angle and group velocity for parallel propagation (to SC2) are also given. The small panel to the right shows (approximately to scale) the relative location of the two spacecraft with respect to the magnetic equator and the source. (b) Similar results for the falling emissions observed on November 27, 2000, at 13:19:29 UT, after the spacecraft crossed the magnetic equator. The small panel to the right shows (approximately to scale) the relative location of the two spacecraft with respect to the magnetic equator and the source.

frequency-time slopes that are observed on SC1 and SC2. The determination of the original frequency range and frequency-time shape of the emission at the source is one of the outcomes of our algorithm, as we search for a source location and speed that is consistent with the frequency-time features of both the SC1 and SC2 observations. Also determined in this process is the specific location at which each frequency is emitted and the velocity (i.e., direction and speed) of the source. Figure 6a shows the calculated source location s_z and source velocity v_s as a function of frequency for the case shown in Figure 4, determined using equations (7), −(12). As expected, there are two possible solutions, one with a source located north of the two spacecraft, and another with the source south of the spacecraft. For comparison, the corresponding values of wave normal angle ψ, refractive index $\mu(\psi)$, and group velocity v_{g0} (for parallel propagation to SC2) are also given. On the wave normal angle plot panel, the corresponding values of the so-called Gendrin angle ψ_G [*Gendrin*, 1974] and the resonance cone angle ψ_R are also shown for reference. Also superimposed on the source velocity plot are the corresponding values of group velocity (for parallel propagation) and the parallel velocity of resonant energetic electrons obtained from equation (4) for $\psi \simeq 0$. We note that the source velocity values for the two possible solutions are nearly identical.

[14] Noting that the source is determined to be moving toward the observing spacecraft, and that the source location varies with frequency, the extent of the source emission region, i.e., the distance between the locations at which the lowest and the highest frequencies are generated, appears to be ∼1500 km, for both of the possible solutions. We further note that the calculated source velocity is of the same order of magnitude (but generally less than) as the wave group velocity and the parallel resonant electron velocity (for $\psi \simeq 0$). Further discussion of the interpretation of source velocity is provided in the next section. While we do not have enough independent evidence to determine which of the two possible source locations is the one from which the particular chorus elements emanate, the solution with the source region closer to the geomagnetic equator is more likely to be the correct one on the basis of past observations indicating that chorus originates from the vicinity of the geomagnetic equator [*LeDocq et al.*, 1998; *Lauben et al.*, 2002]. Even on this basis, however, the two solutions look very similar, with the distance from the geomagnetic equatorial plane at 6 kHz being ∼5000 km in both cases.

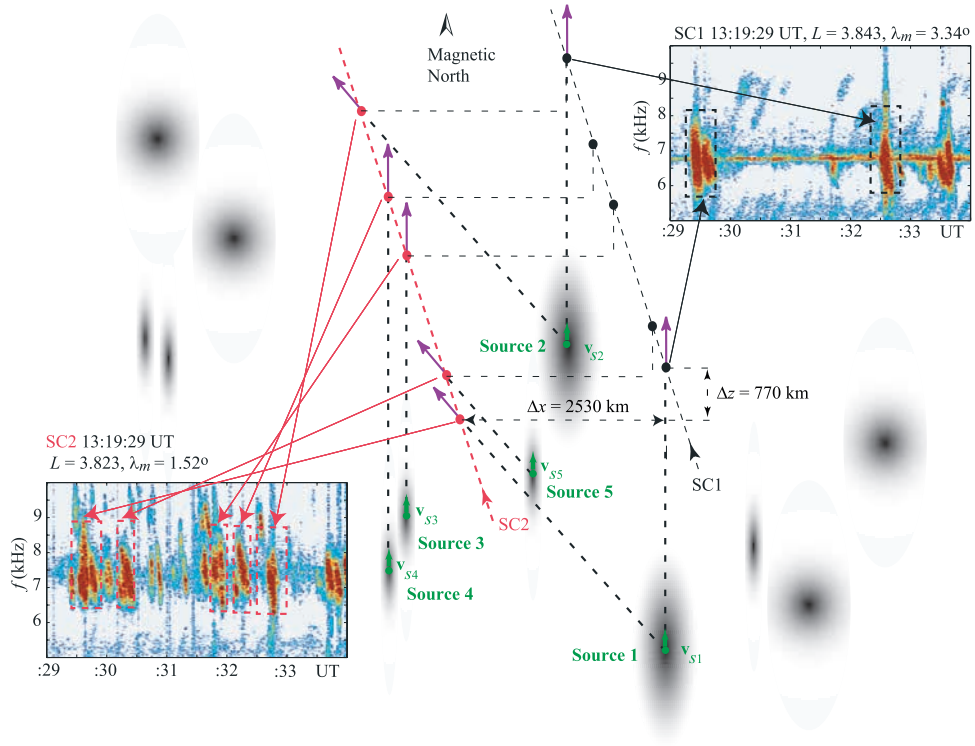

Figure 7. Scheme of the proposed model of different localized sources of ELF/VLF chorus distributed in the region near the spacecraft. Highlighted are the trajectories of spacecraft SC1 and SC2 and the points where the emissions are detected along it. Data from November 27, 2000, are shown as an example, when the same elements are detected on both spacecraft and when they are only detected on one of them.

[15] It is evident from Figures 3 and 4 that although some chorus elements are observed on both spacecraft, others are singularly seen on only one of the satellites. Such is observed to be the case throughout the ~30 minutes of observations on this day, suggesting the presence of a multiplicity of chorus sources, distributed in space, with each spacecraft receiving wave packets in general from different sources, but sometimes also from the same source. This concept of a constantly active and bubbling set of sources feeding signals to different locations is illustrated in Figure 7.

[16] Even in the midst of many chorus elements that are not common to both spacecraft, individual discrete emissions that are observed on both spacecraft can nevertheless be identified, by means of the combination of the unique temporal pattern in which they occur, and/or their distinct frequency-time shapes. Detailed visual analysis of 30-sec long spectrograms from SC1 and SC2 (by printing one record on a transparency and overlaying it on the other one to identify common emissions) was used to measure the variation of differential Doppler shift and time delay as a function of time during the pass, leading to the result shown in Figures 8a and 8b. It is interesting to note that both the differential Doppler shift and the time delay change sign shortly after the crossing of the geomagnetic equator, although such behavior is likely to be a coincidence, since it was not manifested in Case 2 which is analyzed and discussed below. In the case of 27 November 2000, the type of chorus emissions also changed from risers to fallers upon the crossing of the geomagnetic equator, although such a change was not observed in Case 2 (Figures 8c and 8d).

[17] Figure 9 shows the expanded records from a time period after the geomagnetic equator crossing, illustrating the falling emissions and the fact that the differential Doppler shift and time delay have now both reversed in sign. Carrying out a similar analysis for this period leads to the calculated source location and velocities as shown in Figure 6b, with once again two possible solutions. The source region is determined to be moving toward the spacecraft, i.e., in the direction of propagation of the chorus wave packets. The source velocity for the falling emissions observed after the equatorial crossing is rather similar (but somewhat smaller at higher frequencies) in comparison with the riser case shown in Figure 6a. The extent of the source along the field line is also somewhat larger, being ~2000 km, even though the frequency range spanned by the fallers in Figure 9 is less than that for the risers in Figure 4. Of the two possible solutions for this case, the solution with the source region located south of the spacecraft is substantially closer to the geomagnetic equator and may thus be deemed to be the more likely solution on the basis of past work [*LeDocq et al.*, 1998; *Lauben et al.*, 2002].

3.2. Case 2: September 13, 2001

[18] Figure 10a shows frequency-time spectrograms showing chorus emissions observed on the two Cluster spacecraft, referred to as SC1 and SC2, as they crossed

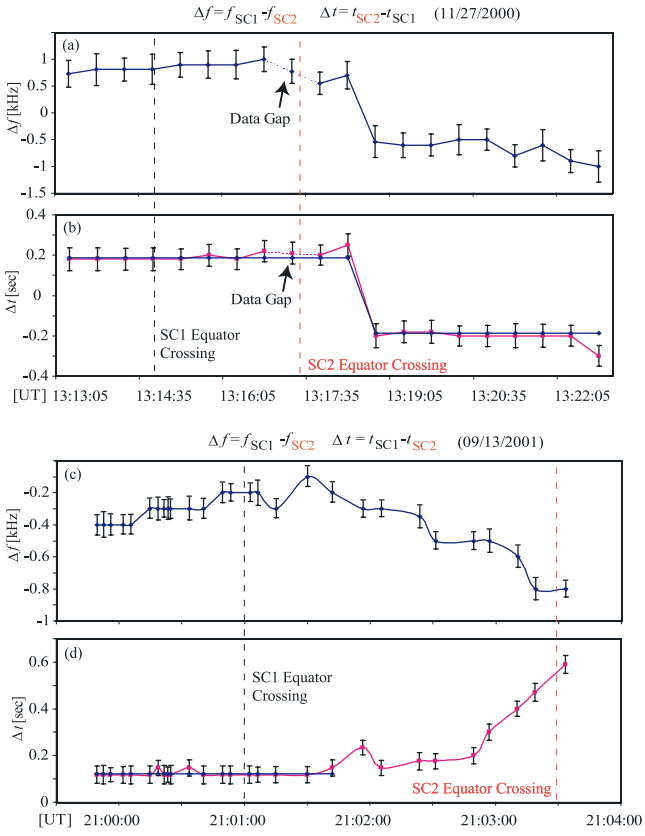

Figure 8. Variation of differential (a) Doppler shift and (b) time delay as a function of time during the November 27, 2000, pass. These two parameters were measured by detailed overlaying (using transparencies) and visual analysis of 30-s-long spectrograms from SC1 and SC2. The error bars correspond to estimated statistical error intrinsic of the measurement method. The same method was applied to the data record measured on September 13, 2001, the results of which are shown in (c) Doppler shift and (d) time delay.

near the geomagnetic equatorial plane on September 13, 2001. The spacecraft separation at the time of this observation was ~840 km, with the precise coordinates of the two spacecraft being as shown in Figures 10b and 10c. Similar to Case 1 (Figure 3) we see that the general variation of the chorus frequency as observed on the two spacecraft are similar, but that the frequency difference is quite evident.

[19] Figure 11 shows an expanded record of a 5-s-long data segment, showing a sequence of individual chorus elements observed on both SC1 and SC2. Once again, the similarity of the temporal sequencing and frequency-time shapes of the emissions strongly suggests a common source, yet the frequency difference of Δf and the time difference (or time delay) of Δt are clearly evident. In fact, careful examination (Figure 12) also reveals that the frequency-time slopes are discernibly different, resulting from the dependence of the dispersion of whistler-mode waves on the wave normal angle ψ.

[20] As in Case 1, our calculation of the source region location and speed accounts for the measurably different frequency-time slope of the individual chorus elements as measured on the two spacecraft (Figure 12). For this case, however, the individual chorus elements are fallers (i.e., frequency decreases with time) so that if the source is determined to be traveling toward (away from) the observers as shown in Figure 12a, the lower frequencies would need to be emitted at points later (earlier) in time, and thus closer to (farther away from) the observers. We note from Figure 11 that chorus emissions are observed earlier on SC1, so that we choose to place the source along the same field line as that spacecraft, although this choice is not as obvious as in Case 1, since the relation between across-the-field-line distance to along-the-field-line distance between the two spacecraft is larger (For Case 1 the ratio of the two distances is 770 km/2530 km $\simeq$ 3/10, while for Case 2 we have 646 km/840 km $\simeq$ 3/4). Nevertheless staying with the choice of the source being located along the same field line as SC1, we next observe that the magnitude of the Doppler shift should be larger as observed on SC2 (since ψ, and thus the magnitude of the **k**-vector, for waves arriving at it are higher) and that the chorus emissions are observed at lower frequencies at SC2, thus indicating that the polarity of the Doppler shift is negative. We thus once again conclude that the source velocity must be directed toward the observing spacecraft.

[21] Carrying out the same analysis as in Case 1, the discrete emission at the source is determined to occur with a linearly decreasing frequency with time (leftmost two panels of Figure 12b), which then disperses (slightly but measurably) to constitute the frequency-time slopes of the falling chorus emissions that are observed on SC1 and SC2. Figure 13 shows the calculated source location s_z and source speed v_s as a function of frequency for the case shown in Figure 11, determined using equations (7)–(12) as described in the previous section. We note that the calculated source velocity is of the same order of magnitude as those found for Case 1 (Figure 6) and are also comparable to both the resonant electron velocities and wave group velocities across the entire range of chorus frequencies. As in Case 1, the source is determined to be moving toward the observing spacecraft. The extent of the source location along the field line, i.e., the distance between the locations at which the lowest and the highest frequencies are generated, is substantially smaller than that for Case 1, being only ~200 km.

[22] Figures 7c and 7d show the variation of differential Doppler shift and time delay as a function of time for this case, measured in the same manner as was described for Case 1 (i.e., using 30-sec overlays of spectrograms from SC1 and SC2). The general appearance of the spectra for this case was similar, consisting of a multiplicity of chorus emissions generally observed only on one spacecraft, in the midst of which were present some elements that were recognized (either on the basis of their disposition in time and/or their distinct frequency-time spectra) to be common to both spacecraft. We see that differential Doppler shift and time delay do not exhibit a polarity reversal in this case but that the magnitude of both Δf and Δt increase as a function of time. In the context of our interpretation, such an increase might result from the spacecraft moving closer to active source regions, in which case the angle ψ_R would grow larger (assuming the spacecraft separation to remain approximately constant), leading to a larger Doppler shift

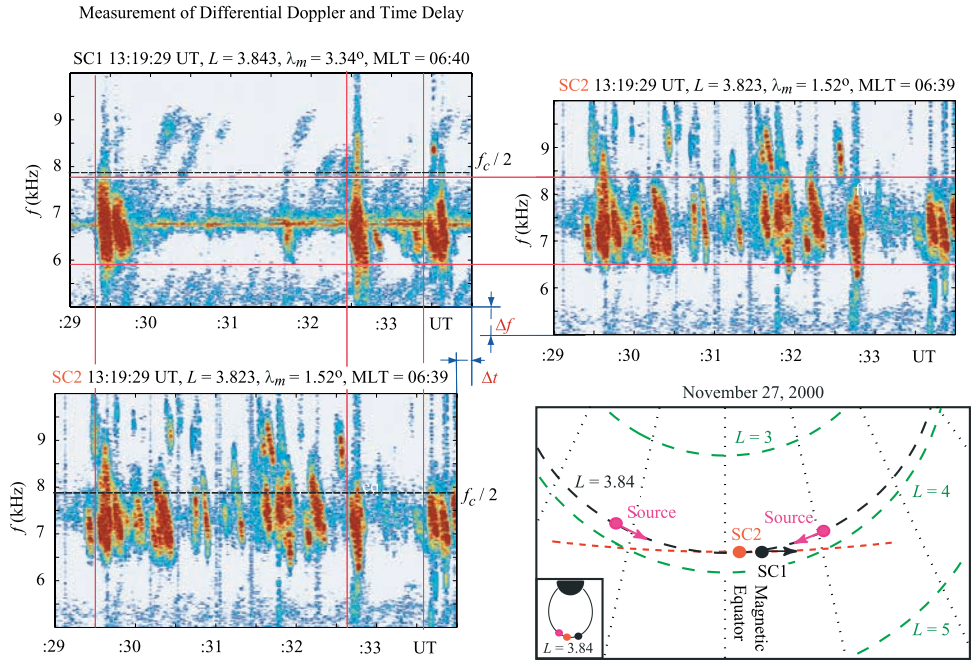

Figure 9. Expanded record of a 5-s-long data segment, starting at 13:19:29 UT, on November 27, 2000, showing a sequence of individual chorus elements observed on both SC1 and SC2. The magnitude scale refers to electric field amplitude with 0 dB corresponding to 1 V/m/$\sqrt{Hz}$. The SC2 panel is repeated on the right to better illustrate the differential Doppler shift. Also shown in the right bottom panel is the location of the spacecraft with respect to the two possible source locations along the field line (as derived from our analysis). The small panel on the left bottom of this diagram shows the entire magnetic field line.

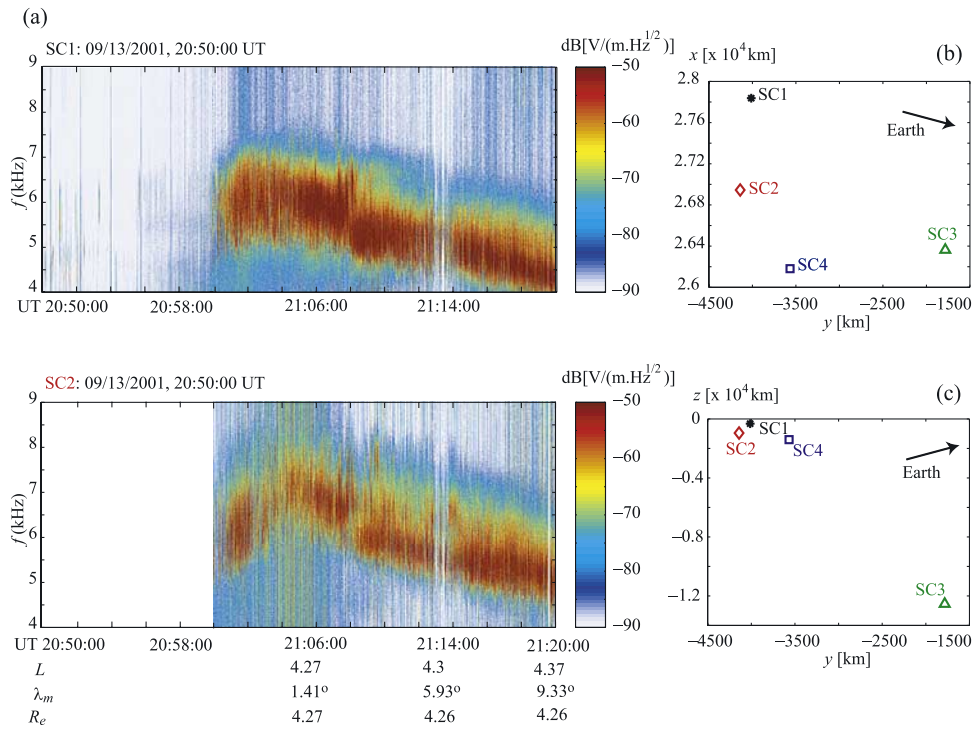

Figure 10. (a) WBD overview spectrogram of the plasma wave data acquired during the Cluster perigee pass on September 13, 2001. The magnitude scale refers to electric field amplitude with 0 dB corresponding to 1 V/m/$\sqrt{Hz}$. Also shown are the relative positions of the four spacecraft with each other and the corresponding distances to Earth (b and c). The x coordinate represents the Earth-Sun axis, while the y coordinate is perpendicular to x, still lying in the Earth's orbit plane. (c) The z coordinate is perpendicular to the Earth's orbit plane.

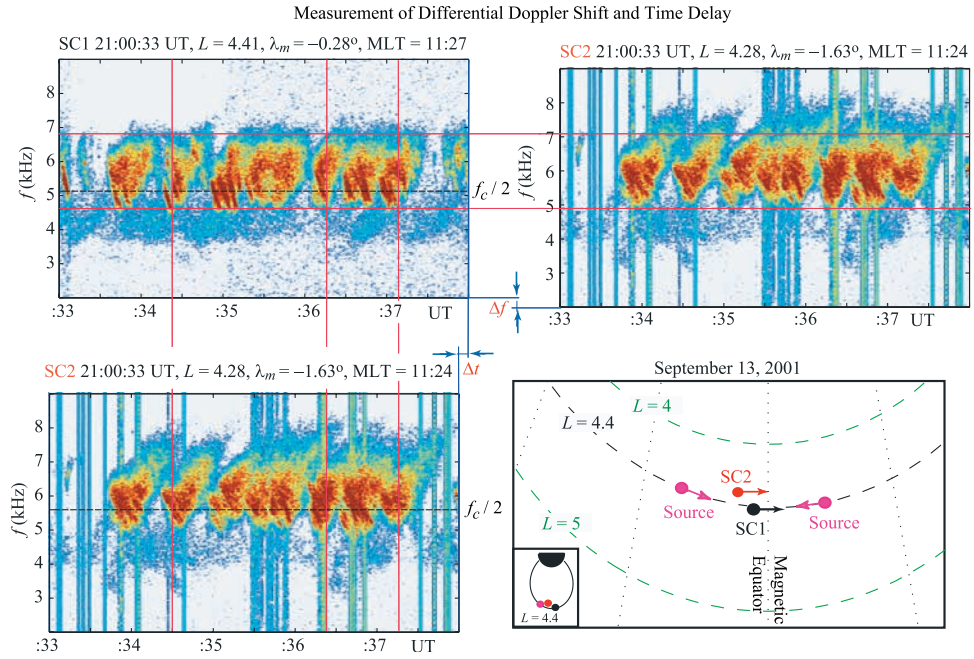

Figure 11. Expanded record of a 5-s-long data segment, starting at 21:00:20 UT, on September 13, 2001, showing a sequence of individual chorus elements observed on both SC1 and SC2. The magnitude scale refers to electric field amplitude with 0 dB corresponding to 1 V/m/$\sqrt{Hz}$. The SC2 panel is repeated on the right to show how the Doppler shift was measured. Also shown in the right bottom panel is the location of the spacecraft with respect to the two possible source locations along the field line (as derived from our analysis). The small panel on the left bottom of this diagram shows the entire magnetic field line.

for the spacecraft which is not located on the field line of the source.

3.3. Case 3: April 18, 2002

[23] We now consider a case in which spacecraft separation is substantially smaller. Figure 14a shows frequency-time spectrograms showing chorus emissions observed on all four of the Cluster spacecraft, referred to as SC1, SC2, SC3, and SC4, as they crossed near the geomagnetic equatorial plane on April 18, 2002. The spacecraft separation at the time of this observation was ~110 km, with the precise coordinates of the four spacecraft shown in Figures 14b and 14c. The general variation of the chorus frequency as observed on the two spacecraft are quite similar and no discernible frequency or time delay differences are evident, even on expanded records shown in Figure 15. This data set was analyzed extensively by *Santolík et al.* [2003] for the purpose of determining the spatial extent of the chorus source regions by cross correlating the chorus waveforms observed on different spacecraft.

[24] As in Cases 1 and 2 (Figures 3 and 10) we see from Figure 14a that the general variation of the chorus frequency as observed on the two spacecraft is similar, but that in this case there are no discernible frequency differences, even in the expanded plots shown in Figure 15. However, we should note here that on the basis of the relatively small separation of the spacecraft, and our discussion above in connection with Figure 1, we expect any differential Doppler shift to be rather small, and that the spectrograms in Figure 14a are necessarily made with a frequency resolution of ~5 Hz. In order to identify any frequency differences that are of order of tens of Hz, we must resort to time-domain analysis.

[25] Figure 15b shows the time-domain waveforms of two individual chorus elements observed on SC1 and SC2, identified with arrows in Figure 15a. The zero-crossings of the waveforms observed at SC1 and SC2 are time-aligned at the beginning of the chorus elements, near 08:47:33.36 UT. As the chorus element develops in time (i.e., its frequency increases), we see that the peaks and zero crossings of the two waveforms (i.e., SC1 and SC2) separate out, in a manner consistent with an inherent difference in the frequencies of the two signals. In fact, counting of the number of peaks in a given time interval on both records indicates that the frequency difference between the chorus elements observed on SC1 and SC2 is approximately half a cycle in ~21 ms, or ~24 ± 1.1 Hz, with SC2 being at a higher frequency. A similar time-domain analysis on all four signals, shown in Figure 15c, indicates that they are all at measurably different frequencies, although some of the signals (e.g., SC3) are not as well defined as others.

4. Discussion

4.1. General Considerations

[26] The results of the three different chorus cases are generally consistent with our hypothesis of rapidly moving chorus source regions, based on Figure 1, in that the differential Doppler shifts (and thus observed frequency differences) are smaller for smaller separation distances between the observing spacecraft. We note, however, that the important determinant here is really not the separation

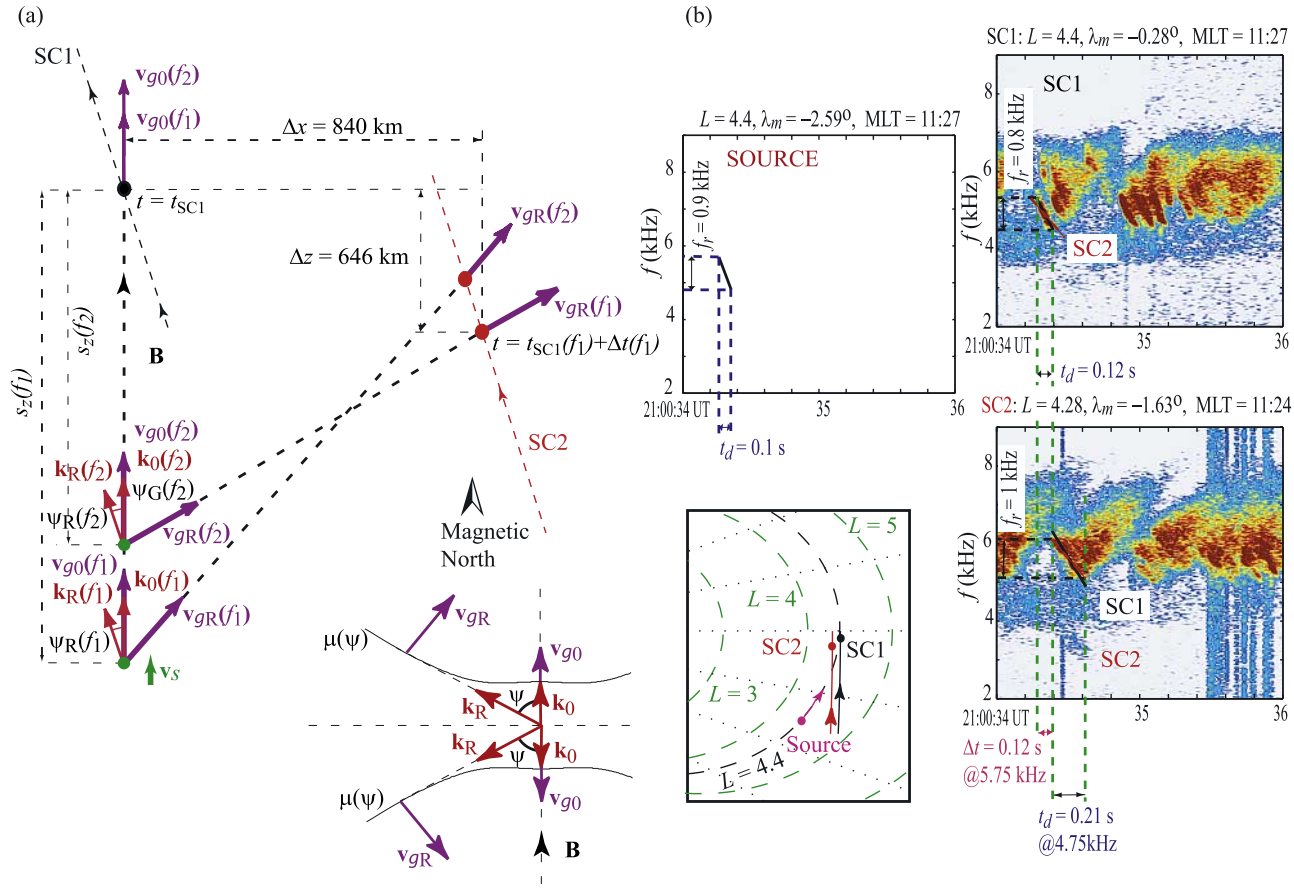

Figure 12. (a) Placement of the source position with respect to the spacecraft and the mechanism of propagation (from source to spacecraft) of the chorus waves, on September 13, 2001, at 21:00:20 UT. Included is a plot of the refractive index surface at different wave normal angle values. (b) Detailed measurement of differential delay and Doppler shift leads to a calculated frequency-time shape at the source as shown in the left panel. This panel shows the results of the calculations of differential Doppler shift and time delay using the calculated values of refractive index and group velocity. Also shown is the location of the spacecraft with respect to the source along the field line.

distance, but rather is the angular range between the line-of-sight distances between a compact source (e.g., point source or one with a spatial extent much smaller than the distance between the two spacecraft and the distance between the spacecraft and the source) and the two observing spacecraft. Figure 16 shows differential Doppler shift Δf and time delay Δt as a function of this angle (labeled β) for different frequencies, and for parameter values that are typical of the geomagnetic equatorial region traversed by Cluster during its perigee passes, of which Cases 1 through 3 were examples. The Δf and Δt values shown here were calculated in a manner described in previous sections, using assumed values of source speed of $v_s = 5 \times 10^4$ km/s and a separation distance of d = 2500 km. The corresponding refractive index values are shown in the lower panel. Superimposed on Figure 16 are the parameter ranges corresponding to Cases 1, 2, and 3 discussed in the previous section. We see that the differential Doppler shift and time delay values observed in these three cases are in good agreement with our general expectations on the basis of the dependence of these quantities on the angle β between the line of sights from the source to the two observers. Note in the upper panel that the curve for $f = 9$ kHz does not follow a regular progression relative to those $f = 7$ kHz and $f = 8$ kHz. This behavior is a direct result of the unique characteristics of the whistler-mode refractive index surface.

[27] In all of our discussion in this and previous sections, we have been presuming that the source regions of discrete chorus emissions are highly compact in the direction transverse to the magnetic field line. It is clear from Figure 2, for example, that if the transverse extent of the source of any particular discrete chorus emission element was comparable to the transverse separation distance (Δy), then the wave normal angles of waves arriving at SC1 and SC2 would be similar, thus resulting in negligible differential Doppler shift. The fact that a differential Doppler shift was measured (in the three cases discussed) thus implies that the transverse extent Δs_y of individual sources must have been substantially less than the smallest of the transverse separations involved, or that $\Delta s_y \ll 100$ km. To further quantify the transverse extent of the source regions, we note that any finite extent ($\perp$ to $\mathbf{B}_0$) of source region(s) limits the observability of chorus in planes $\perp$ to $\mathbf{B}_0$, independent of accessibility issues due to limited group velocity directions.

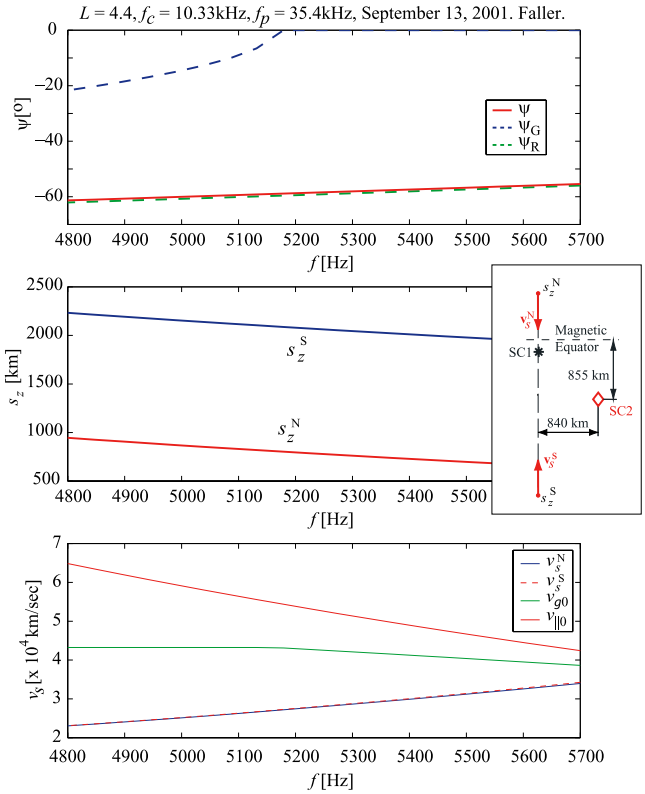

Figure 13. Results of the calculations of the source location and source velocity as a function of frequency for the cases on September 13, 2001, at 21:00:20 UT. Shown are the two solutions, one with a source located north of the spacecraft and another with the source located south of the spacecraft. The corresponding values of wave normal angle and group velocity for parallel propagation (to SC2) are also given. The small panel to the right shows (approximately to scale) the relative location of the two spacecraft with respect to the magnetic equator and the source.

Assume, for example, source currents (which radiate the chorus emissions) pointing in the same direction distributed over a circular region of radius $r = a$ ($\perp$ to $\mathbf{B}_0$). Assume further that, the radiation produced at any given time (at a given frequency) originates from radiating currents distributed only over a distance of $\Delta z \ll \lambda$ along $\mathbf{B}_0$, where λ is the wavelength along $\mathbf{B}_0$. The currents within the circular region represent an array of sources of electromagnetic waves, with an array factor:

$$F(\theta) = \int_0^a J_0(kr\sin\theta)rdr = \frac{aJ_1(ka\sin\theta)}{k\sin\theta} \qquad (15)$$

where $J_0(\cdot)$ and $J_1(\cdot)$ are the Bessel functions of order zero and one, and β is the angle of the observation point with respect to $\mathbf{B}_0$. The electromagnetic power radiated at angle β is modulated by $[F(\beta)]^2$, the -3dB point for its main lobe being at $k\,a\,\sin\beta \simeq 2$. The radiation beam halfwidth is $\beta \simeq \sin^{-1}(2/\pi) \simeq 40°$, for $a \simeq \lambda$, and $\beta \simeq 4°$ for $a \simeq 10\lambda$. Observation of significant differential Doppler shifts on the Cluster spacecraft can thus generally occur only if the source region radius a is of order of a wavelength λ or less. This result agrees with *Santolík et al.* [2003], who came to the conclusion that since the source is so small, the radiation must extend over a large range of wave normal angles.

[28] In our study we have not attempted to use the amplitude of the chorus elements as a predictor of source location for two reasons. First, because of the fact that the magnitude of the whistler-mode Poynting vector is dependent on the wave normal angle, amplitude differences can occur even when the distance from the source and the observer is kept constant. Second, the chorus elements are produced via a gyroresonance instability, and the net gain (or growth) in this process may depend on the wave normal angle, and may thus lead to amplitude differences at an observer even when the distance to the source is constant. Because of these uncertainties the chorus amplitudes were not used in our analysis. However, consideration of these amplitudes would indeed be important is testing the predictions of models of the actual chorus generation and amplification process.

4.2. Interpretation of Source Motions

[29] In the context of our interpretation of the Cluster observations, discrete chorus emissions are produced in source regions which are highly compact (of order a wavelength or tens of kilometers) in the direction transverse to the magnetic field, but which are extended by as much as a few hundred kilometers along the magnetic field so that different frequencies are emitted at different points along the field line. In the cases studied here, the source regions are found to be moving toward the observers (i.e., in the direction of the wave packets), for both rising and falling emissions. Motion of the source (or interaction) region in the direction of wave propagation and at the speed corresponding to the wave group velocity corresponds to an equilibrium condition in which no power flows out of the interaction region so that a minimal amount of energy needs to be supplied by new counterstreaming electrons to supply energy to the wave [*Helliwell*, 1967]. Such an equilibrium can exist under conditions of marginal levels of electron flux and anisotropy, with the motion of the region optimizing the emitted wave power. If, on the other hand, the particle flux (and/or anisotropy) is very high, the interaction region would be expected to drift in the direction of the counterstreaming electrons at speeds approaching that of the parallel velocity of the resonant electrons [*Helliwell*, 1967]. In our cases, we find the speed with which the sources move to be of the same order but somewhat less than the wave group velocities, consistent with somewhat better than marginal conditions for wave amplification and growth.

[30] The frequency-time shapes of the chorus elements as they are emitted at the source were determined as part of our analyses for Cases 1 and 2. In Case 1, the source region for riser emissions observed during the earlier time before the spacecraft crossed the magnetic equator was found to lie on the downstream side (with respect to particle motion, so that 'downstream' means along the particle parallel velocity or in the direction opposite to the wave propagation direction) of the geomagnetic equator. This finding is consistent with the generation of emissions with rising frequency, if we simply consider the cyclotron resonance equation (4) for a given particle, when the increasing gyrofrequency as seen by the electrons, is compensated by the increasing wave

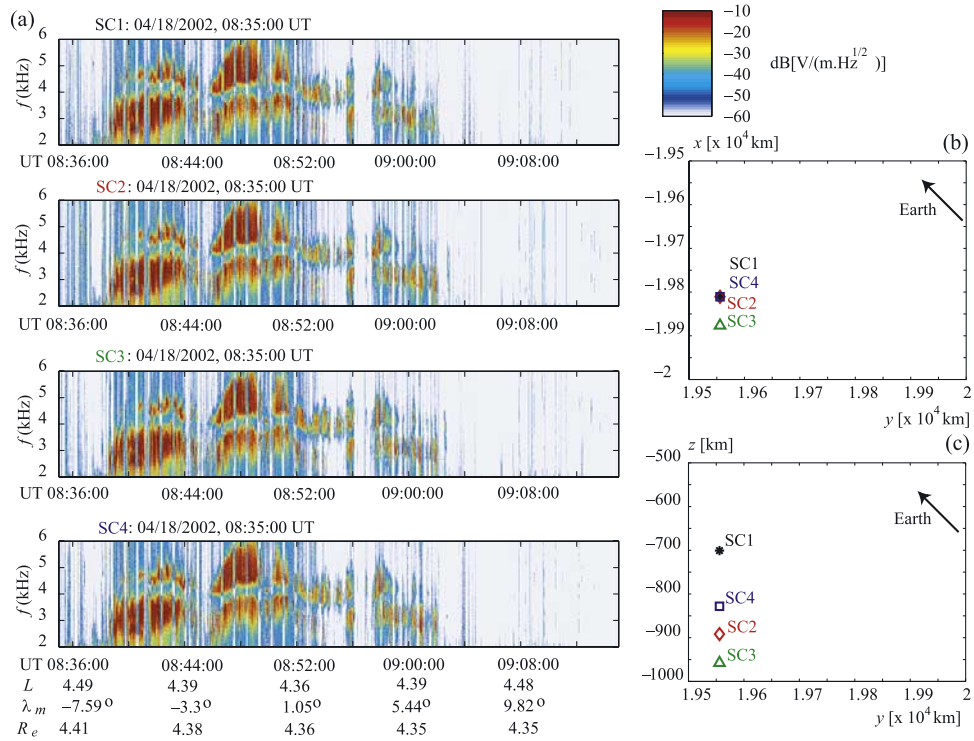

Figure 14. (a) WBD overview spectrogram of the Cluster perigee pass on April 18, 2002. The magnitude scale refers to electric field amplitude with 0 dB corresponding to 1 V/m/$\sqrt{Hz}$. The Cluster WBD instrument was set to record magnetic field data from the antenna [*Gurnett et al.*, 1997] for ~10 s every minute which correspond to the vertical streaks during which the background levels are different. Also shown are the relative positions of the four spacecraft with each other and the corresponding distances to Earth (b and c). The x coordinate represents the Earth-Sun axis, while the y coordinate is perpendicular to x, still lying in the Earth's orbit plane. (c) The z coordinate is perpendicular to the Earth's orbit plane.

frequency. This compensation would tend to enhance the total duration of time in which individual electrons can remain resonant with the wave. On the other hand, since we find the source region to drift in the direction of the wave, and thus closer to the equator (i.e., decreasing gyrofrequency), one might mistakenly deduce from equation (4) that the frequency should increase. However, such would only be true if the parallel velocity $v_{||}$ remained constant, or if the emission were produced by the same single beam of energetic electrons. In fact, however, the chorus emission is likely produced by the collective interaction with the wave of electrons distributed in both parallel velocity and pitch angle [e.g., *Nunn et al.*, 1997, and references therein], so that the fact that a rising emission is observed cannot be uniquely related to the location of the source region with respect to the equator, without detailed information about the energetic particle distribution function. In other words, the frequency-time shape of the emission, i.e., the fact that it is a riser or a faller, is likely not due to the location (with respect to the equator) of the source region, or even its motion, but is rather determined by the particular distribution function in effect at the time. In terms of the relationship of the chorus generation region to the geomagnetic equator, it should be further noted that in all the three cases discussed herein, the K_p index during the hours preceding the chorus observations were >4,5 (September 13, 2001, and November 27, 2000, respectively), and >6 (April 18, 2002), so that there may well have been multiple geomagnetic equators (i.e., a minima in $\mathbf{B}_0$), as is in fact quite evident from Figure 1 of *Santolík et al.* [2003], showing a record of ω_c along the satellite pass. Accordingly, our sketches of satellite and source locations in Figures 6 and 13 should be viewed simply as first approximations, especially in terms of their relationship to the geomagnetic equator.

5. Comparison With Other Recent Work

[31] *Santolík and Gurnett* [2003] and *Santolík et al.* [2003] have used the chorus observations on April 18, 2002 (i.e., our Case 3), to determine the extent of the chorus source region using the temporal correlation between discrete elements received on all four Cluster spacecraft. The source region in their work was assumed to be stationary, and the transverse extent of source is deduced on the basis of the temporal correlation between the chorus waveforms observed on different spacecraft. Their estimates of source regions of ~35 km half-width in the direction transverse to the magnetic field and extending for ~2000 km along the field line is consistent with the range of values derived in our analysis of Cases 1 and 2. Note that the differential Doppler shifts were too small for us to extract source region velocity or size for Case 3. It is also interesting to note that *Santolík et al.* [2003] showed (in

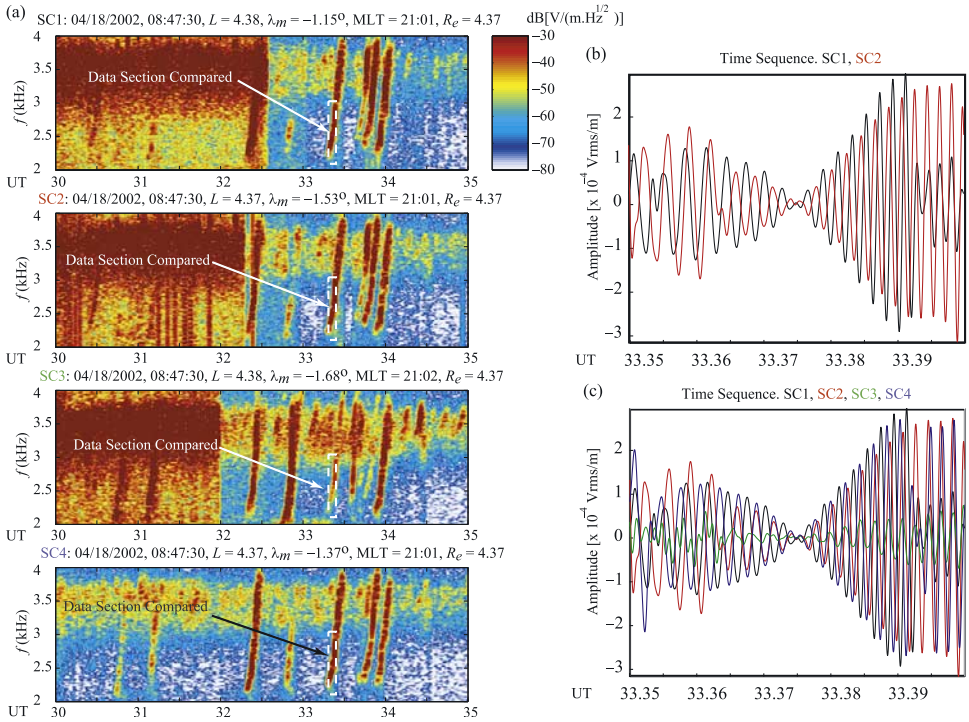

Figure 15. Expanded record of a 5-s-long segment, starting at 08:47:30 UT, in April 18, 2002, showing a sequence of individual chorus elements observed on SC1, SC2, SC3, and SC4. The magnitude scale refers to electric field amplitude with 0 dB corresponding to 1 V/m/$\sqrt{Hz}$. The second half of each of the top three spectrograms and all of the SC4 spectrogram shows data acquired with the magnetic antenna. The sharp amplitude transition in the data from the spacecraft SC1, SC2, and SC3 corresponds to the antenna switch from the electric to the magnetic. The dB scale used for the magnetic field data has been kept the same as that for the electric field so that magnetic field data should be viewed as relative (uncalibrated) values. Also shown is the time domain waveform of the signal portion highlighted in the spectrogram. The data were filtered around the highlighted frequencies and translated to baseband to be shown as a time series.

Figure 1d of their paper) that chorus elements for this case had wave normal angles mostly near zero, but that close to the nominal equator wave normal angles up to ~75 could occur. Thus our use of high wave normal angles (for waves arriving at one of the two spacecraft) is not inconsistent with *Santolík et al.* [2003]. Nevertheless it should be noted that the wave normal angles quoted there were determined from magnetic field measurements from the Spatio-Temporal Analysis of Field Fluctuations (STAFF) instrument [*Cornilleau-Wehrlin et al.*, 1997], and the resulting angles there were very small. It should also be noted that *Santolík et al.* [2003] used mostly data from the electric-field antenna in their analyses, whereas in our measurement of the differential Doppler shift (Figure 15) we use wave magnetic field measurements. In this particular case, the magnetic field data is cleaner (i.e., larger signal-to-noise ratio) although it is available for less of the time, and is thus suited for our single point measurements. In their correlation analyses of longer records of data, *Santolík et al.* [2003] used the electric field data, and possibly for this reason did not resolve the ~24 Hz differential Doppler shift that we have inferred (Figure 15).

[32] *Lauben et al.* [2002] undertook a detailed analysis of the source characteristics of ELF/VLF chorus based on observations on the POLAR spacecraft, at locations substantially removed from the equatorial source regions. Using 6-channel (three magnetic and three electric components) wideband waveform data, these authors were able to use the frequency dependent group dispersion and the measured wave normal angles together with backward ray tracing to determine the location of the chorus source regions. Their findings indicate that chorus emissions generally originate within a few degrees of the geomagnetic equator, and at wave normal angles $\psi = \psi_G$ for $\omega < \omega_c/2$ and $\psi = 0$ for $\omega > \omega_c/2$, where ψ_G is the so-called Gendrin angle [*Gendrin*, 1974] at which the whistler-mode refractive index surface exhibits an inflection (see Figure 1) such that the direction of the wave group velocity is along the magnetic field. For the cases analyzed here, and generally for the relatively low density regions outside the plasmapause in which chorus is observed, the Gendrin angle is not too close to the resonance cone angle, and the magnitude of the refractive index at $\psi = \psi_G$ is not too different from that at $\psi = 0$. Thus, although in our analyses we have for simplicity considered the waves observed on the spacecraft along the same field line as the source to emanate at $\psi = 0$, our results (i.e., the source locations and velocities derived) do not substantially change if we were to assume these waves to instead emanate at $\psi = \psi_G$. In terms of assessing our results in the light of those of *Lauben et al.* [2002], it is not

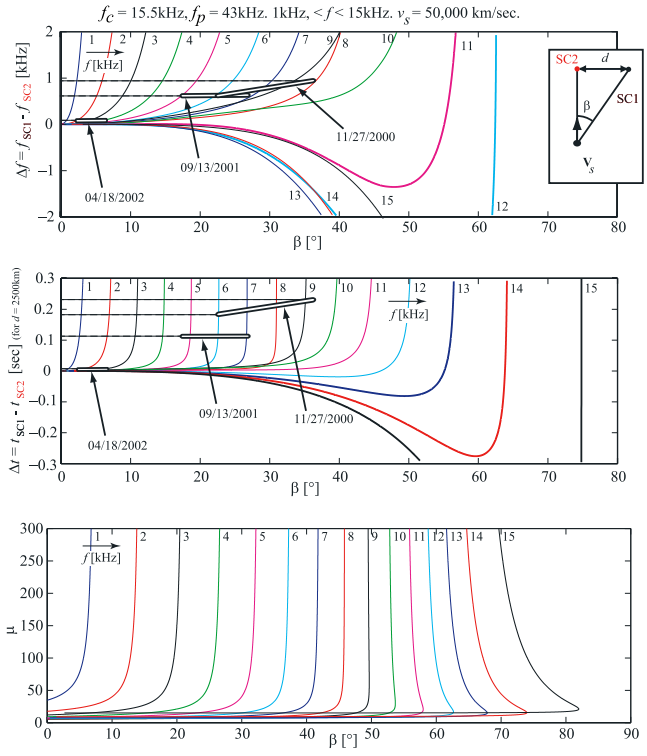

Figure 16. Differential Doppler shift and time delay as a function of the angle β between the line-of-sight distances from a compact source to the two observing spacecraft for different frequencies, and for parameter values that are typical of the geomagnetic equatorial region traversed by Cluster during the November 27, 2000, September 13, 2001, and April 18, 2002, passes. Also included are the calculated refractive index values as a function of the angle β and frequency. The small panel to the right shows the geometry used. Notice that the vertical distance between SC1 and SC2 is not used.

possible for us to distinguish between the two possibilities of chorus being emitted at relatively high angles between the Gendrin angle and the resonance cone or at a continuum of angles between zero and the resonance cone. Such a determination is fortunately not essential for the primary purpose of this paper, which is to establish the rapid motion of the chorus source regions.

[33] The overall picture of many simultaneously active compact chorus source regions, bubbling all the time and constantly in rapid motion is not inconsistent with past observations, since spacecraft located away from the geomagnetic equator would in general only be receiving waves emanating from one or a small group of co-located source regions at any given time. With observations on a single spacecraft, and without a fixed frame of reference, it would not have been possible to determine the magnitude of the Doppler shift of the observed chorus signals. On the basis of the results of the cases discussed in this paper, the absolute values of the Doppler shifts range from ~2 kHz to ~8 kHz. This new realization raises some questions concerning the identification of chorus bands based on their relationship to the equatorial value of ω_c. For example chorus often appears in two frequency bands one above, and one below, $\omega_c/2$. The two bands are separated by a gap at $\omega \simeq \omega_c/2$ [*Anderson and Maeda*, 1977]. For a compact chorus source, the center frequency of the band corresponding to the gap would be a function of the spacecraft position with respect to the source. This effect would tend to weaken the correlation of the center frequency of the gap with $\omega_c/2$.

6. Summary

[34] The initially surprising observation of frequency differences between individual discrete chorus elements observed on different Cluster spacecraft is naturally explained in terms of Doppler shifts resulting from rapid motion of chorus source regions. Rapid motion is consistent with counterstreaming gyro-resonant electrons being the source of waves. The magnitude of observed differential Doppler shift and time delay are consistent with theoretical predictions for the different spacecraft separations. Source velocities are comparable to the particle parallel velocity or the wave group velocity. In both of the two examples considered here, the source regions were determined to be moving toward the observers for both falling tone emissions (Case 2) and rising tones (Case 1), indicating convection of the region of maximum radiation in the direction of the emanating waves. Discrete chorus emissions appear to be produced in source regions that are compact (~λ or less) in the direction perpendicular to $\mathbf{B}_0$. Different frequencies of individual discrete chorus elements are emitted at different points (separated by 200 km to 1500 km) along the field line. Multiple, simultaneously active source region(s) are likely spread out in L-shell and longitude (as well as in latitude) and continually emitting waves.

[35] Our results in this paper constitute the first experimental evidence of the fact that source regions that emit discrete chorus waves are in rapid motion. This finding should provide important guidance to theoretical efforts aimed at better understanding of the mechanisms of generation of these intense discrete emissions.

[36] **Acknowledgments.** This research was supported by the National Aeronautics and Space Administration, under parent grant NAG5-9974 at the University of Iowa and with Subcontract 4000061641 to Stanford University. We greatly appreciate the help of C. Abramo of DSN and M. Hapgood of RAL in scheduling the real-time wideband data acquisition from the WBD receiver, and also the help of J. H. Dowell, I. W. Christopher, J. M. Seeberger, and R. L. Brechwald of the University of Iowa in reducing the data to usable form. We thank P. Décréau and P. Canu, who have provided the WHISPER data. We also thank J. Yarbrough, who was instrumental in the initial analysis of the data for the November 27, 2000, case.

[37] Lou-Chuang Lee thanks Vikas S. Sonwalkar and Michel Parrot for their assistance in evaluating this paper.

References

Anderson, R. R., and K. Maeda (1977), VLF emissions associated with enhanced magnetospheric electrons, *J. Geophys. Res.*, *82*, 135–146.

Cornilleau-Wehrlin, N., et al. (1997), The CLUSTER Spatio-Temporal Analysis of Field Fluctuations (STAFF) Experiment, *Space Sci. Rev.*, *79*, 107–136.

Gendrin, R. (1974), Phase-bunching and other non-linear processes occurring in gyroresonant wave-particle interactions (in magnetosphere), *Astron. Space Sci.*, *28*, 245–266.

Gurnett, D. A., W. S. Kurth, and F. L. Scarf (1979a), Plasma wave observations near Jupiter: Initial results from Voyager 2, *Science*, *206*, 987–991.

Gurnett, D. A., R. R. Anderson, F. L. Scarf, R. W. Fredricks, and E. J. Smith (1979b), Initial results from the ISEE 1 and 2 plasma wave investigation, *Space Sci. Rev.*, *23*, 103–122.

Gurnett, D. A., R. L. Huff, and D. L. Kirchner (1997), The Wide-Band Plasma Wave Investigation, *Space Sci.*, *79*, 195–208.

Gurnett, D. A., R. L. Huff, J. S. Pickett, A. M. Persoon, C. A. Kletzing, R. L. Mutel, I. W. Christopher, U. S. Inan, W. L. Martin, and J. L. Bougeret (2001), First results from the Cluster Wide-Band Plasma Wave Investigation, *Ann. Geophys.*, *19*, 1259–1272.

Helliwell, R. A. (1965), *Whistlers and Related Ionospheric Phenomena*, Stanford Univ. Press, Stanford, Calif.

Helliwell, R. A. (1967), A theory of discrete VLF emissions from the magnetosphere, *J. Geophys. Res.*, *72*, 4273–4790.

Inan, U. S., Y. T. Chiu, and G. T. Davidson (1992), Whistler mode chorus and morningside aurorae, *Geophys. Res. Lett.*, *19*, 653–656.

Lauben, D. S., U. S. Inan, T. F. Bell, D. Kirchner, G. B. Hospodarsky, and J. S. Pickett (1998), VLF chorus emissions observed by POLAR during the January 10, 1997, magnetic cloud, *Geophys. Res. Lett.*, *25*, 2995–2998.

Lauben, D. S., U. S. Inan, T. F. Bell, and D. A. Gurnett (2002), Source characteristics of ELF/VLF chorus, *J. Geophys. Res.*, *107*(A12), 1429, doi:10.1029/2000JA003019.

LeDocq, M. J., D. A. Gurnett, and G. B. Hospodarsky (1998), Chorus source locations from VLF Poynting flux measurements with the Polar spacecraft, *Geophys. Res. Lett.*, *25*, 4063–4066.

Nunn, D., Y. Omura, H. Matsumoto, I. Nagano, and S. Yagitani (1997), The numerical simulation of VLF chorus and discrete emissions observed on the Geotail satellite using a Vlasov code, *J. Geophys. Res.*, *102*(A12), 27,083–27,098.

Santolík, O., and D. A. Gurnett (2003), Transverse dimensions of chorus in the source region, *Geophys. Res. Lett.*, *30*(2), 1031, doi:10.1029/2002GL016178.

Santolík, O., D. A. Gurnett, J. S. Pickett, M. Parrot, and N. Cornilleau-Wehrlin (2003), Spatio-temporal structure of storm-time chorus, *J. Geophys. Res.*, *108*(A7), 1278, doi:10.1029/2002JA009791.

Scarf, F. L., D. A. Gurnett, and W. S. Kurth (1979), Jupiter plasma wave observations: An initial Voyager 1 overview, *Science*, *204*, 991–995.

Smith, A., M. Freeman, and G. Reeves (1996), Postmidnight VLF chorus events, a substorm signature observed at the ground near $L = 4$, *J. Geophys. Res.*, *101*(A11), 24,641–24,654.

Stix, T. H. (1962), *The Theory of Plasma Waves*, McGraw-Hill, New York.

Warwick, J. W., et al. (1979), Voyager 1 planetary radio astronomy observations near Jupiter, *Science*, *204*, 995–998.

T. F. Bell, U. S. Inan, and M. Platino, STAR Laboratory, Stanford University, Stanford, CA 94305, USA. (inan@stanford.edu)

D. A. Gurnett and J. S. Pickett, Department of Physics and Astronomy, University Of Iowa, Iowa City, IA 52242, USA.